Metal-specific CD4$^+$ T-cell responses induced by beryllium exposure in HLA-DP2 transgenic mice

MT Falta[1], AN Tinega[1], DG Mack[1], NA Bowerman[1], F Crawford[2,3], JW Kappler[2,3], C Pinilla[4] and AP Fontenot[1,2]

Chronic beryllium disease (CBD) is a granulomatous lung disorder that is associated with the accumulation of beryllium (Be)-specific CD4$^+$ T cells into the lung. Genetic susceptibility is linked to *HLA-DPB1* alleles that possess a glutamic acid at position 69 (βGlu69), and *HLA-DPB1*02:01* is the most prevalent βGlu69-containing allele. Using HLA-DP2 transgenic (Tg) mice, we developed a model of CBD that replicates the major features of the human disease. Here we characterized the T-cell receptor (TCR) repertoire of Be-responsive CD4$^+$ T cells derived from the lungs of Be oxide–exposed HLA-DP2 Tg mice. The majority of Be-specific T-cell hybridomas expressed TCR Vβ6, and a subset of these hybridomas expressed identical or nearly identical β-chains that were paired with different α-chains. We delineated mimotopes that bind to HLA-DP2 and form a complex recognized by Be-specific CD4$^+$ T cells in the absence of Be. These Be-independent peptides possess an arginine at p5 and a tryptophan at p7 that surround the Be-binding site within the HLA-DP2 acidic pocket and likely induce charge and conformational changes that mimic those induced by the Be^{2+} cation. Collectively, these data highlight the interplay between peptides and Be in the generation of an adaptive immune response in metal-induced hypersensitivity.

INTRODUCTION

Chronic beryllium disease (CBD) is a classic example of a human disorder resulting from gene-by-environment interactions. Genetic susceptibility to CBD is linked to HLA-DP alleles that contain a glutamic acid at the sixty-ninth position of the β-chain (βGlu69),[1] with the prevalence of βGlu69-expressing HLA-DP alleles ranging from 73 to 95% of CBD patients.[2–6] In addition, the probability of CBD increases with HLA-DP βGlu69 copy number and increasing workplace exposure to beryllium (Be).[7] Depending on genetic susceptibility and exposure, CBD develops in up to 18% of Be-exposed workers.[1,8–10] The disease is characterized by granulomatous inflammation and an influx of T helper type 1–polarized CD4$^+$ T cells that express a differentiated memory T-cell phenotype[11–13] and an oligoclonal T-cell receptor (TCR) repertoire.[14,15] Importantly, the vast majority of Be-specific CD4$^+$ T cells recognize antigen in an HLA-DP-restricted manner,[16,17]

and the HLA-DP molecules that mediate Be presentation match those implicated in disease susceptibility. These findings confirm that the mechanism of HLA contribution to disease susceptibility is based on the ability of those molecules to bind and present Be to pathogenic CD4$^+$ T cells.[16,17]

We recently developed an HLA-DP2 transgenic (Tg) murine model of Be-induced disease.[18] Intratracheal exposure of these mice to Be oxide (BeO) induced mononuclear cell infiltrates in the lung and a Be-specific adaptive immune response in the lung and spleen that was CD4-dependent and HLA-DP2-restricted. Using Be-loaded HLA-DP2 tetramers expressing either mimotope 2 or plexin A4 peptides,[19] we identified a population of lung CD4$^+$ T cells in HLA-DP2 Tg mice that recognized the same TCR ligands as CD4$^+$ T cells derived from the bronchoalveolar lavage (BAL) of CBD patients. Thus this murine model replicates the major features of the human disease and proves that expression of a single major

histocompatibility complex (MHC) class II (MHCII) molecule in a previously resistant mouse drives disease development upon environmental exposure to Be.

Here we determined the TCR gene sequences expressed by Be-responsive CD4$^+$ T cells derived from the lungs of BeO-exposed HLA-DP2 Tg mice and investigated the spectrum of peptides that permit Be recognition by a subset of these TCRs. The TCR repertoire of these Be-responsive clones was dominated by the expression of Vβ6 TCRs that were composed of identical or related complementarity determining region 3 (CDR3) sequences. We utilized a positional scanning peptide library[19–22] to screen a Vα4/Vβ6-expressing T-cell transfectoma to determine whether the peptides required to complete the αβTCR ligand possessed similar Be-coordinating amino-acid residues as was previously observed for human Be-specific TCRs.[19] As opposed to the identification of Be-dependent mimotopes,[19] we identified mimotopes that stimulated the Be-specific T-cell transfectomas in the absence of Be. These Be-independent mimotopes expressed arginine (R) and tryptophan (W) residues at the p5 and p7 positions of the peptide, respectively. We speculate that these distinct amino acids near the Be-binding site induce similar changes in charge and conformation to the HLA-DP2-peptide complex as those induced by the addition of the Be^{2+} cation.

RESULTS

Expansion of Vβ6$^+$ CD4$^+$ T cells in the lung and BAL of BeO-exposed HLA-DP2 transgenic mice

To characterize the TCR repertoire of CD4$^+$ T cells present in the lung and spleen of HLA-DP2 Tg FVB/N mice, we pooled the lung and spleen cells from 10 mice and determined the percentage of CD4$^+$ T cells expressing particular TCR Vβ chains using immunofluorescence staining (**Figure 1**). Because the FVB/N strain is characterized by a large genomic deletion in the *TCRB* gene locus,[23] we focused on the limited set of expressed Vβs shown in **Figure 1a**. We noted an increased

percentage of CD4$^+$ T cells expressing Vβ6 in the BAL and lung of BeO-exposed mice (**Figure 1a,b**). For example, compared with 11.1% of CD4$^+$ T cells in the lungs of unexposed mice, 13.4% and 16.8% of lung and BAL CD4$^+$ T cells, respectively, expressed Vβ6 (**Figure 1b**). In addition, when gating on blasting (large forward scatter) T cells compared with a small lymphocyte gate (**Figure 1c**), the
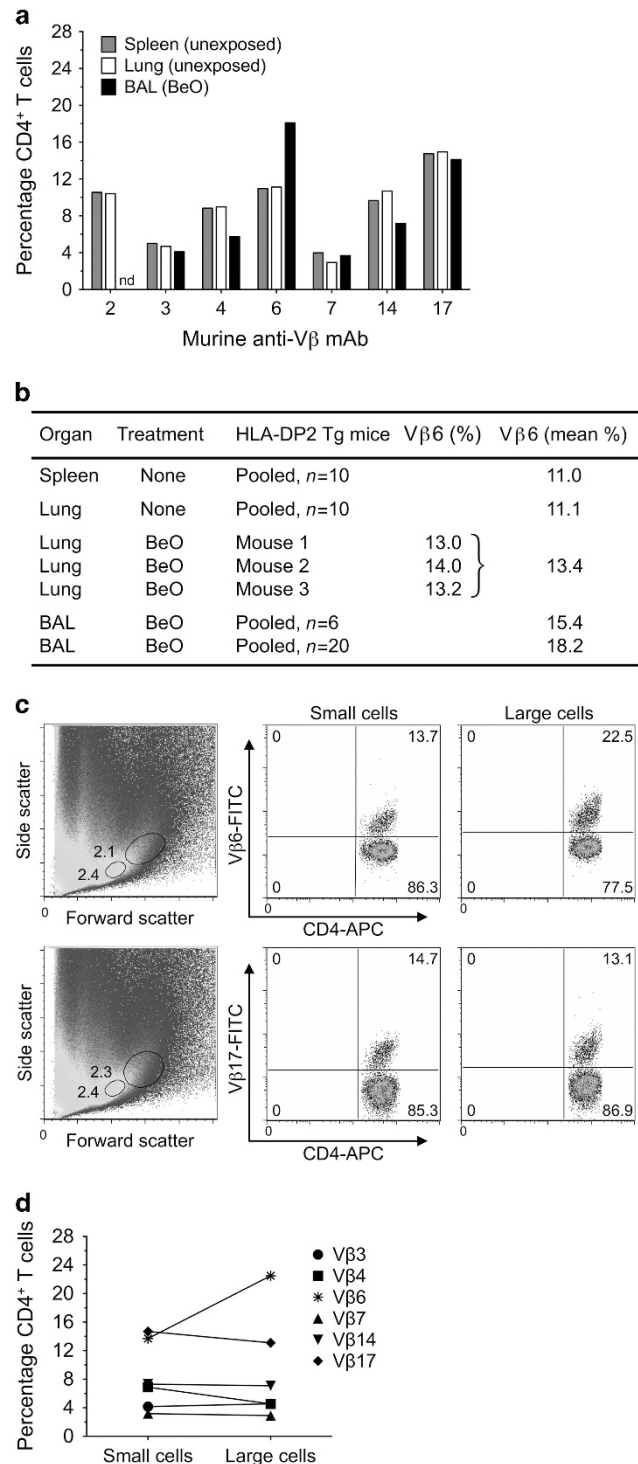

Figure 1 T-cell receptor (TCR) Vβ repertoire of CD4$^+$ T cells in HLA-DP2 Tg FVB/N mice. (**a**) Percentage of CD4$^+$ T cells expressing particular TCR Vβ-chains are shown for pooled lung and spleen cells ($n=10$) from untreated HLA-DP2 Tg mice and pooled bronchoalveolar lavage (BAL) cells ($n=20$) isolated from HLA-DP2 Tg mice exposed to beryllium oxide (BeO). Monoclonal antibodies (mAbs) chosen were based on the known genomic deletion within the *TCRB* locus of FVB/N mice and the availability of anti-TCR Vβ reagents. The seven mAbs in the panel account for >60% of the total Vβ repertoire. ND, not determined (**b**) Summary of CD4$^+$ T-cell expression of Vβ6 in different cell populations of untreated or BeO-exposed HLA-DP2 Tg mice. BAL cells from multiple treated mice were pooled in order to have enough cells to perform the analysis. (**c**) Representative density plots of CD4/Vβ6 (top plots) and CD4/Vβ17 (bottom plots) staining of BAL T cells obtained by pooling cells from 20 BeO-exposed HLA-DP2 Tg mice are shown. Forward by side scatter plots (left) were used to gate small and blasting lymphocyte populations and compare Vβ expression within each subset. In the CD4/Vβ plots, the number in the upper right quadrant indicates the percentage of CD4$^+$ T cells expressing the particular Vβ. (**d**) Summary of the frequency of CD4$^+$ T cells expressing particular Vβs in small and blasting (large) lymphocyte gates. Data show that Vβ6 is the only T-cell population enriched in the blasting T-cell population compared with small lymphocytes.

frequency of CD4$^+$ T cells expressing Vβ6 increased from 13.7% to 22.5% of BAL cells from 20 BeO-exposed HLA-DP2 Tg mice (**Figure 1c,d**). This distribution between blasting and small lymphocytes contrasted to other TCR Vβ subsets that either decreased in frequency or remained unchanged (**Figure 1c,d**). Collectively, these findings suggested that Vβ6$^+$ CD4$^+$ T cells are expanded in the lung and BAL after BeO exposure and may contain Be-responsive T cells.

TCR gene expression of Be-specific T-cell hybridomas derived from the lungs of BeO-exposed HLA-DP2 Tg mice
We have previously shown that the Be-specific adaptive immune response in BeO-exposed HLA-DP2 Tg mice is CD4$^+$ T cell dependent.[18] To characterize this Be-specific T-cell population, the lungs from 10 BeO-exposed HLA-DP2 Tg mice were harvested, and the pooled cells were stimulated *in vitro* with 10 μM BeSO$_4$. Blasting T cells were purified and expanded in interleukin (IL)-2 prior to fusing with TCR α$^-$/β$^-$ BW5147 thymoma cells. Of 90 T-cell hybridomas screened for Be specificity, 29 were Be-responsive and secreted IL-2 after BeSO$_4$ exposure using an HLA-DP2-expressing murine fibroblast cell line as antigen-presenting cells (data not shown).

To determine *TCR* gene usage for each of the hybridomas, panels of *TCRAV* and *TCRBV* primers were used with TCR constant region primers to screen hybridoma cDNA by PCR. As shown in **Figure 2a**, *TCRAV4* and *TCRBV6* were the most commonly utilized V gene segments, being expressed in 45% and 55% of the Be-responsive hybridomas, respectively. *TCRAV* and *TCRBV* gene segment usage and CDR3 amino-acid sequences of all of the Be-responsive T-cell hybridomas are displayed in **Figure 2b**. Among the TCR Vβ6-expressing hybridomas, a CDR3β motif was evident in a subset of five hybridomas, utilizing different nucleotides to encode identical or nearly identical amino-acid sequences with conserved CDR3 length and *TCRBJ* gene usage (**Figure 3**). As some of the Vβ6-expressing hybridomas expressed multiple TCR α-chains (**Figure 2b**) and considering the genetic instability of the hybrids, we generated immortalized T-cell transfectomas for each of the TCRs shown in **Figure 3**. For transfectoma LB9-18, the accompanying α-chain that conferred Be specificity was *TCRAV4S2* while the correct α-chain for LB10-17 was *TCRAV1S1* (see **Supplementary Figure S1** online). Similar to Be-specific TCRs derived from the lungs of CBD patients,[24,25] the oligoclonal Vβ6 chains were paired with different α-chains (**Figure 3**). Using these transfectomas in T-cell-stimulation assays, their ability to respond to BeSO$_4$

in vitro was equivalent to that of a Be-specific TCR (AV22) derived from the lungs of a CBD patient (**Figure 4a**).
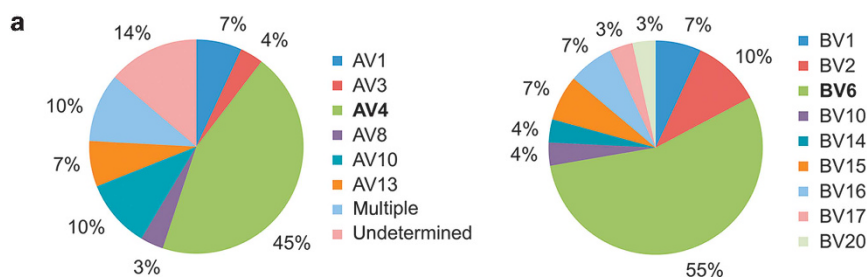
We have previously shown that TCR recognition of the HLA-DP2-peptide/Be complex by human CD4$^+$ T cells requires glutamic acid (E) residues at positions 26, 68, and 69 of the HLA-DP2 β-chain.[26,27] For the human TCR AV22 and five murine T-cell transfectomas, amino-acid substitutions at these positions of the HLA-DP2-peptide/Be complex abrogated Be-induced IL-2 secretion (**Figure 4b**). Thus these Be-specific TCRs derived from BeO-exposed HLA-DP2 Tg mice recognize the HLA-DP2-peptide/Be complex in a similar manner as TCRs derived from humans with CBD. The only difference was that AV22 had a partial reduction in IL-2 secretion with the EA68 HLA-DP2 β-chain variant while this mutation abolished the response of the murine TCRs (**Figure 4b**).

TCR gene expression of Be-specific T-cell hybridomas that recognize the HLA-DP2-PLXNA4/Be complex
We previously demonstrated that a subset of lung CD4$^+$ T cells from BeO-exposed mice recognized Be-loaded HLA-DP2 tetramers with either mimotope 2 or plexin A4 peptide in the peptide-binding groove,[18,19] the same TCR ligands found in CBD patients. Interestingly, all of the TCRs expressed on the Be-specific hybridomas in the current study, with the exception of LBM10-13, failed to bind either of these tetramers (data not shown). Using a T-cell transfectoma expressing the AV22 TCR as a positive control for tetramer co-staining, **Figure 5** shows that LBM10-13 bound to the HLA-DP2-plexinA4/Be tetramer but not to a Be-loaded HLA-DP2 tetramer expressing the highly related peptide, mimotope 2. The amino-acid sequence of the plexin A4 epitope is FVDDLFETIF while that of mimotope 2 is FWIDLFELIG.[19] Conversely, LB11-3 did not bind either Be-loaded HLA-DP2-peptide tetramer. Thus only one of the 29 Be-responsive T-cell hybridomas derived from the lung of BeO-exposed HLA-DP2 Tg mice was specific for the HLA-DP2-plexinA4/Be complex.

To identify additional CD4$^+$ T cells specific for this αβTCR ligand, lung cells from BeO-exposed HLA-DP2 Tg mice were stained with the HLA-DP2-PLXNA4/Be tetramer, and positively staining cells were sorted for direct TCR sequencing. As shown in **Figure 6a**, we identified αβTCR pairs for three CD4$^+$ T cells. Interestingly, two of the three were highly related to LBM10-13 that was identified in our initial screen, and both of these Vβ16$^+$ TCRs (scG-1 and scE-1) utilized *TCRAV4S9* with differing n and *AJ* regions (**Figure 6a**). To confirm antigen

Figure 2 T-cell receptor (TCR) gene expression of beryllium (Be)-specific T-cell hybridomas. (**a**) Pie charts show the frequency of *TCRAV* (left) and *TCRBV* (right) gene segment usage of 29 Be-specific T-cell hybridomas derived from the lungs of Be oxide–exposed HLA-DP2 transgenic mice. (**b**) Shown are *TCR* gene segment usage and junctional region amino-acid sequences of Be-specific T-cell hybridomas. Identified *TCRB* and *TCRA* V and J gene segments are indicated using the nomenclature of Arden *et al*.[39] In some instances, precise V gene segment usage (ND) or subfamily usage (nd) could not be assigned. Also presented are the deduced CDR3 amino-acid sequences of the *TCRB* and *TCRA* genes beginning at the conserved cysteine (C) of the expressed V gene segment and ending at the conserved phenylalanine-glycine (FG) of the J gene segment. Two pairs of hybridomas (LB9-18/LB10-9 and LBM10-10/LB11-9) were duplicate clonal isolates sharing identical nucleotide sequences. In four instances, two functional *TCRA* genes were obtained for an individual hybridoma. The correct TCR α/β chain pair conferring Be specificity (denoted by an asterisk) was determined for three of these hybridomas by separately expressing the TCRs on recipient hybridoma cell lines and testing for Be-specificity by interleukin-2 enzyme-linked immunosorbent assay.

a

Left pie chart (AV): 7% AV1, 4% AV3, 45% **AV4**, 3% AV8, 10% AV10, 7% AV13, 10% Multiple, 14% Undetermined

Right pie chart (BV): 7% BV1, 10% BV2, 55% **BV6**, 4% BV10, 4% BV14, 7% BV15, 7% BV16, 3% BV17, 3% BV20

b

Hyb	BV	Vβ	NDβN	Jβ	BJ	AV	Vα	N	Jα	AJ
LB12–17	1S1	CASS	QLTDTS	YAEQFFG	2S1	4S9	CAL	SST	ASLGKLQFG	24
LB10–7	1S1	CASS	QTGNF	YEQYFG	2S7	4.nd	CA	P	NNAGAKLTFG	39
LB9–13	2S1	CSAD	HLGG	YAEQFFG	2S1	13S1	CAA	SV	YNVLYFG	21
LB12–3	2S1	CSAD	HRGG	AETLYFG	2S3	13S1	CAA	S	NYNVLYFG	21
LB12–4	2S1	CTCS	AAGGAR	AETLYFG	2S3	4S2	CAL	GEG	DSGTYQRFG	13
LB11–3	3S1	CASS	LGRA	NTLYFG	1S3	4S9	CAL	SL	NTGNYKYVFG	40
LB9–17	6S1	CASS	LNA	NTEVFFG	1S1	ND				
LB11–4	6S1	CASS	RTNS	YNSPLYFA	1S6	10S3	CAM	E	NMGYKLTFG	9
LBM9–5	6S1	CASS	RQGL	NSPLYFA	1S6	10S3	CAM	DR	DTNAYKVIFG	30
LB11–2	6S1	CASS	STGGWD	AEQFFG	2S1	4S11	C	VL	GTGGYKVVFG	12
LB9–18	6S1	CASS	ILGG	QNTLYFG	2S4	4S2*	CAL	Q	SSGSWQLIFG	22
						13S1	CAA	RR	NNYAQGLTFG	26
LB10–9	6S1	CASS	ILGG	QNTLYFG	2S4	4S2*	CAL	Q	SSGSWQLIFG	22
						13S1	CAA	RR	NNYAQGLTFG	26
LBM10–10	6S1	CASS	ILGG	QNTLYFG	2S4	4S9	CAL	S	SSGSWQLIFG	22
LB11–9	6S1	CASS	ILGG	QNTLYFG	2S4	4S9	CAL	S	SSGSWQLIFG	22
LB10–17	6S1	CASS	ILGG	QNTLYFG	2S4	1S1*	CAV	T	TGGADRLT G	45
						10S6	C	ARL	SNTDKVVFG	34
LBM12–1	6S1	CAS	TRLGG	QNTLYFG	2S4	1S3	CAVS	P	SGSWQLIFG	22
LBM11–8	6S1	CASS	RLGG	QDTQYFG	2S5	1S3	CAVS		TGGADRLTFG	45
LBM11–1	6S1	CASS	IRGGY	QDTQYFG	2S5	3.nd	CAVS	P	MGYKLTFG	9
LBM9–1	6S1	CAS	RGGG	DTQYFG	2S5	10.nd	CAM	L	SSGSWQLIFG	22
LB9–5	6S1	CAS	RQG	DTQYFG	2S5	4S9	CAL	SP	SGGSNAKLTFG	42
LB10–16	6S1	CASS	WTGP	DTQYFG	2S5	ND				
LBM9–18	14S1	CAWS	PGTN	SGNTLYFG	1S3	ND				
LB9–14	15S1	CGAR	GTGS	SQNTLYFG	2S4	4S11	CVL	GERA	GNTRKLIFG	37
						4.nd	CAL	GA	YAQGLTFG	26
LB10–12	15S1	CGAA	GTGGL	QDTQYFG	2S5	ND				
LBM9–13	16S1	CASS	LKGG	QNTLYFG	2S4	4S9	CAL	TS	NTGYQNFYF	49
LBM10–13	16S1	CASS	LGGR	NTQYFG	2S5	4S9	CAL	SP	NTGYQNFYFG	49
LB11–8	17S1	CASS	PRGG	YNSPLYFA	1S6	3.nd	CAVS	AD	YGGSGNKLIFG	32
						20S1	CAA	V	NSGGSNYKLTFG	53
LBM9–4	20.nd	CSS	RPRQGWD	TEVFFG	1S1	4S2	CAL	R	ATGGNNKLTFG	56
LBM10–21	ND					8S3/S9	CALS	DGG	GSALGRLHFG	18

Clone	BV6S1	NBDN	BJ2S4	AV use
LB9–18	91 C A S S TGT GCC AGC AGT	95 I L G G ATA CTG GGA GGG	99 Q N T L Y F G CAA AAC ACC TTG TAC TTT GGT	AV4S2
LBM10–10	C A S S TGT GCC AGC AGT	I L G G ATT CTG GGG GGG	Q N T L Y F G CAA AAC ACC TTG TAC TTT GGT	AV4S9
LB10–17	C A S S TGT GCC AGC AGT	I L G G ATT CTG GGG GGC	Q N T L Y F G CAA AAC ACC TTG TAC TTT GGT	AV1S1
LBM11–8	C A S S TGT GCC AGC AGT	R L G G CGA CTG GGG GGT	Q D T Q Y F G CAA GAC ACC CAG TAC TTT GGG	AV1S3
LBM12–1	C A S T TGT GCC AGC ACC	R L G G CGA CTG GGG GGC	Q N T L Y F G CAA AAC ACC TTG TAC TTT GGT	AV1S3

Figure 3 T-cell receptor (TCR) CDR3β nucleotide and deduced amino-acid sequences from a related set of beryllium-specific Vβ6.1[+] T-cell hybridomas. Variations in nucleotide and deduced amino-acid sequence compared with hybridoma LB9-18 are underlined. Note that hybridoma LBM11-8 expresses *TCRBJ2S5*; the others in this set express *BJ2S4*. Also indicated is *TCRAV* gene use for each hybridoma. The cysteine (C) of the β-chain is designated as amino-acid position 91 with the NβDN and the Jβ region beginning at positions 95 and 99, respectively.

Figure 4 T-cell transfectoma response to beryllium (Be). (**a**) Select T-cell transfectomas were stimulated with an equal number of HLA-DP2-transfected fibroblasts (designated 8302) as antigen-presenting cells and various amounts of $BeSO_4$ (0.3–300 μM) in fetal bovine serum–containing medium. Interleukin (IL)-2 secretion (mean ± s.e.m. pg ml^{-1}) was measured by enzyme-linked immunosorbent assay after 22 h of culture, and data were plotted as the percentage of maximum IL-2 secretion against $BeSO_4$ concentration. Mean EC_{50} values (concentration of $BeSO_4$ that results in a half-maximal T-cell transfectoma response) (μM) for each transfectoma were determined by nonlinear regression of the activation curves using Prism software (GraphPad). The AV22 transfectoma, expressing a human Vβ5.1[+]/Vα22[+] TCR derived from lung of a chronic beryllium disease patient[24] is shown for comparison. Dose–response curves are representative of three independent experiments carried out in triplicate. (**b**) Be-induced IL-2 secretion (pg ml^{-1}) by AV22 and the five murine Vβ6[+] T-cell transfectomas in response to $BeSO_4$ presentation by fibroblasts expressing either wt HLA-DP2 or HLA-DP2 variants with alanine (A), glutamine (Q), or lysine (K) substitutions at positions 26, 68, and 69 of the β-chain is shown.

specificity, we expressed these TCRs on an α⁻β⁻ immortalized cell line.[24] Each of the TCRs was confirmed to be Be-specific and recognized the HLA-DP2-plexinA4/Be complex as demonstrated by tetramer staining (**Figure 6b**) and IL-2 secretion (**Figure 6c**). Similar to LBM10-13, none of these transfectomas bound the HLA-DP2-mimotope-2/Be tetramer (data not shown). Finally, the Be-specific TCR (scC-6) that stained with the highest affinity (highest mean fluorescent intensity) also responded to the addition of PLXNA4/Be with greatest IL-2 secretion (i.e., lowest EC_{50} value, defined as the peptide concentration inducing a half-maximal IL-2 response) (**Figure 6b,c**).

Identification of TCR ligands using a decapeptide positional scanning library

As the specific peptides required for T-cell recognition of Be remained unknown for the vast majority of murine Be-specific TCRs, we utilized an unbiased decapeptide positional scanning library to systematically assess all peptides of a given length in a standard T-cell activation assay.[19] We focused on LB9-18 as a representative of the set of Be-specific Vβ6[+] T-cell transfectomas expressing related oligoclonal TCRs (**Figure 3**). A surprisingly limited number of mixtures with particular amino acids fixed at certain positions of the peptide stimulated the LB9-18 TCR above background (**Figure 7a**). Specifically, the peptide mixtures that induced >20 pg ml^{-1} IL-2 secretion in the presence of $BeSO_4$ contained a glycine (G) at the p2 position, methionine (M) at p3, serine (S) at p4, arginine (R) and leucine (L) at p5, leucine (L) at p6, tryptophan (W) at p7, and tyrosine (Y) at p8 (**Figure 7a**). No definitive selection of amino acids was seen at the p1, p9, and p10 positions, although a possible preference for nonpolar amino acids (isoleucine (I) and valine (V)) was observed at p9.

Based on the preferences of the LB9-18 TCR for particular amino acids at each position of the peptide (**Figure 7b**), we synthesized a set of 14 mimotopes, also choosing to include mimotopes with a phenylalanine (F) at p1 as this amino-acid is a preferred anchor residue for HLA-DP2 at this position[19,28] (**Figure 8a**). These peptides were tested for their ability to
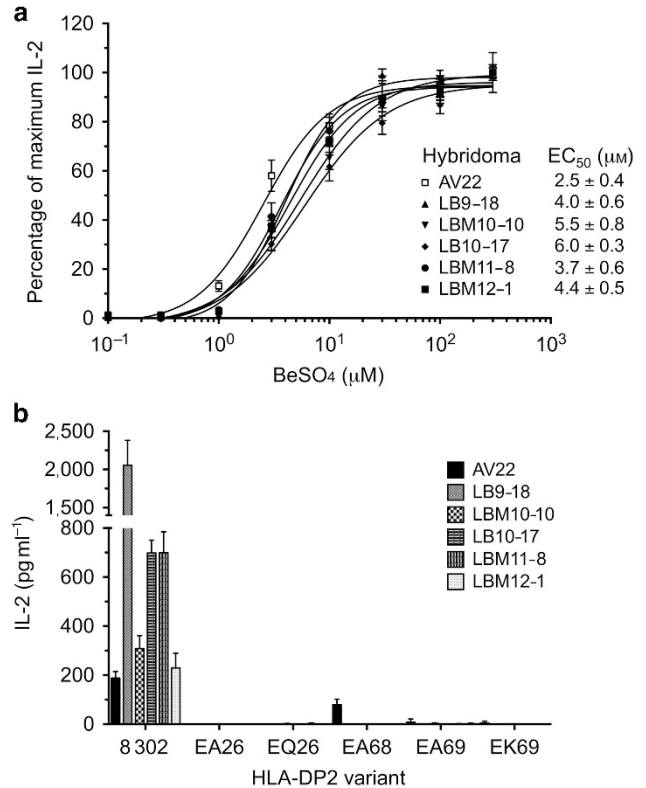
stimulate the Be-specific T-cell transfectomas. In **Figure 8a**, mimotopes were ranked based on IL-2 secretion by transfectoma LB9-18 with mimotopes 6, 5, 13, 7, 9, and 1 stimulating T-cell activation and IL-2 secretion. However, only mimotopes 5, 6, and 13 induced IL-2 secretion at the lowest peptide concentration tested (0.5 μg ml^{-1}; **Figure 8a**). Interestingly, these mimotopes were Be independent as they stimulated IL-2 secretion by the T-cell transfectomas in the absence of $BeSO_4$ (LB9-18 shown in **Figure 8b**). As mimotopes 5 and 6 only differed at the p1 position (T vs. F), we focused on mimotope 6. T-cell transfectoma LBM10-10 responded to mimotope 6 in a similar manner as LB9-18 with EC_{50} values of 3.7 ± 0.2 and 6.8 ± 0.6 μM, respectively (**Figure 8c**). Conversely, LB10-17 responded less well (dose–response curve shifted to

the right; $EC_{50} = 26 \pm 8.0\,\mu M$) (**Figure 8c**), and LBM11-8 and LBM12-1 did not respond at all (data not shown).

To determine the critical amino acids for either mimicking Be or interacting with the TCR, alanine (A) substitutions of mimotope 6 at positions p2, p3, p4, p5, p7, and p8 were synthesized and tested in the absence of Be. We chose not to alter p1 and p6 as these are known anchor residues[19,28] and we could directly compare mimotopes 6 and 5 (T vs. F at p1). In

addition, as no obvious amino-acid selection was seen at p9 and p10 and as we have previously shown that Be-specific TCRs do not contact these positions,[19,29] we did not further investigate p9 and p10. Using T-cell transfectoma LB9-18, an F-to-T substitution at p1 of the peptide shifted the dose–response curve to the right, resulting in an 11-fold increase in the EC_{50} value (**Figure 9**, upper panel). Alanines at the p3, p5, or p7 positions abrogated T-cell recognition of the HLA-DP2-peptide/Be complex while A at p2, p4, or p8 had minimal effects on activation of the LB9-18 transfectoma (**Figure 9**, upper panel). LB9-18 and LB10-10 had a similar response to the alanine variants (**Figure 9**, middle panel). Conversely, LB10-17 had a 14-fold increase in EC_{50} values for mimotope 6 and the variants and did not recognize the mimotope 6 A4 variant (**Figure 9**, lower panel).

Compared with **Figure 4b** where glutamic acids at positions 26, 68, and 69 of the HLA-DP2 β-chain were required for Be-induced T-cell activation of LB9-18 and LBM10-10, the addition of the Be-independent mimotope 6 eliminated the requirement for an E at position 26 (see **Supplementary Figure S2**). In addition, the presence of the isomorphic Q at this position enhanced IL-2 secretion by the transfectomas as compared with an A. Importantly, an E at positions 68 and 69 remained required even in the presence of mimotope 6 (see **Supplementary Figure S2**).
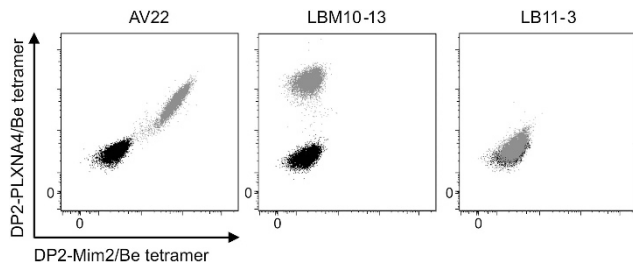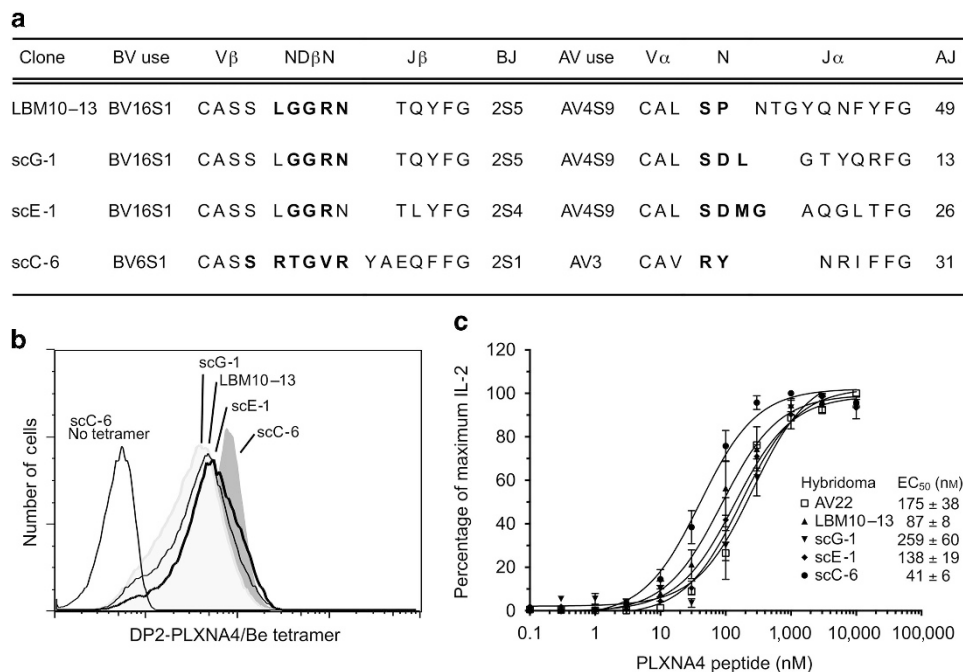

Figure 5 HLA-DP2-peptide/beryllium (Be) tetramer staining of Be-responsive T-cell transfectomas. Co-staining of three Be-specific transfectomas (AV22, LBM10-13, and LB11-3) with Be-saturated HLA-DP2-mimotope-2 (BV421-labeled) and HLA-DP2-PLXNA4 (phycoerythrin-labeled) tetramers (shown in gray) compared with unstained cells (shown in black). Representative results from three independent experiments are shown.

Clone	BV use	Vβ	NDβN	Jβ	BJ	AV use	Vα	N	Jα	AJ
LBM10–13	BV16S1	C A S S	**L G G R** N	T Q Y F G	2S5	AV4S9	C A L	**S P**	N T G Y Q N F Y F G	49
scG-1	BV16S1	C A S S	**L G G R** N	T Q Y F G	2S5	AV4S9	C A L	**S D L**	G T Y Q R F G	13
scE-1	BV16S1	C A S S	**L G G R** N	T L Y F G	2S4	AV4S9	C A L	**S D M G**	A Q G L T F G	26
scC-6	BV6S1	C A S **S**	**R T G V R**	Y A E Q F F G	2S1	AV3	C A V	**R Y**	N R I F F G	31

Figure 6 Characterization of HLA-DP2-PLXNA4/beryllium (Be)-specific murine T cells. (**a**) Shown are T-cell receptor (TCR) gene segment usage and junctional region amino-acid sequences of CD4^{+} T cells specific for the HLA-DP2-PLXNA4/Be complex. LBM10-13 was derived by fusing T cells from the lung of beryllium oxide–exposed HLA-DP2 Tg mice to α[−]/β^{−} BW5147 thymoma cells to generate a TCR-expressing hybridoma. The other TCRs were identified by 5' rapid amplification of cDNA ends and PCR from CD4^{+} CD44^{+} T cells that were individually sorted by flow cytometry for binding to the HLA-DP2-PLXNA4/Be tetramer (phycoerythrin-labeled). Each antigen-specific TCR was subsequently expressed as transfectomas for subsequent analyses. (**b**) Representative staining of T-cell transfectomas with the HLA-DP2-PLXNA4/Be tetramer is shown. (**c**) Dose–response curves to PLXNA4 peptide were completed on the four murine-derived T-cell transfectomas and human transfectoma AV22 for comparison. Various amounts of peptide (0.1 nM–10 μM) and 75 μM $BeSO_4$ were added to wells containing equal numbers of transfectoma cells and DP2.21 fibroblasts. Interleukin (IL)-2 secretion (pg ml^{-1}) was measured by enzyme-linked immunosorbent assay after 22 h of culture, and data are plotted as the percentage of maximum IL-2 against peptide concentration in the presence of $BeSO_4$. EC_{50} values (nM) are shown, and results are representative of three independent experiments.

DISCUSSION

CBD results from Be exposure in the workplace and the subsequent development of an adaptive immune response to the metal.[30] Our previous studies have characterized the TCR repertoire[14,15] and binding topology[24,25] of Be-specific CD4^{+} T cells derived from the blood and BAL of humans with CBD. In addition, recent analyses of the structure and function of

HLA-DP2 in the context of CBD have shown that glutamic acid residues at positions 26, 68, and 69 of the HLA-DP2 β-chain are required for successful Be presentation to T cells,[27] and the function of these amino acids is to capture and coordinate the Be^{2+} cation.[29] Although Be does not directly interact with the TCR, the addition of the Be^{2+} cation induces both charge and conformational changes to the HLA-DP2-peptide complex that are subsequently recognized as a neoantigen.[29] Here we characterized the TCR repertoire of Be-responsive CD4^{+} T cells in an HLA-DP2 Tg murine model of CBD[18] and identified CD4^{+} T cells specific for the HLA-DP2-PLXNA4/Be complex. In addition, we identified Be-independent mimotopes for a set of highly related Vβ6-expressing CD4^{+} T cells derived from the lungs of BeO-exposed HLA-DP2 Tg mice. Collectively, our findings expand our understanding of the interplay between Be and HLA-DP2-bound peptide in the generation of Be-induced hypersensitivity.

The ability of murine T cells to fuse with an immortal thymoma line enabled the characterization of TCRs derived from 29 Be-specific T cells, a quantity that far exceeds the total number of Be-specific T-cell clones derived from CBD patients. Using an unbiased combinatorial peptide library approach, we identified mimotopes that stimulated Be-specific Vβ6^{+} CD4^{+} T-cell transfectomas in the absence of Be. In contrast to previously identified Be-dependent mimotopes that possessed negatively charged aspartic and glutamic acid residues at the p4 and p7 positions of the peptide,[19] these mimotopes were composed of a positively charged R at p5 and a bulky W at p7. Despite the differences, similar features included the preference for F at p1 and the absence of any significant selection for particular amino acids at the carboxy end of the peptide. An F at p1 has been shown by our group[19] and others[28] to be the preferred anchoring amino-acid in the P1 pocket of HLA-DP2 while the lack of selection at the peptide carboxy end is likely due to the focus of the TCR on the center of the HLA-DP2-peptide complex.[29]
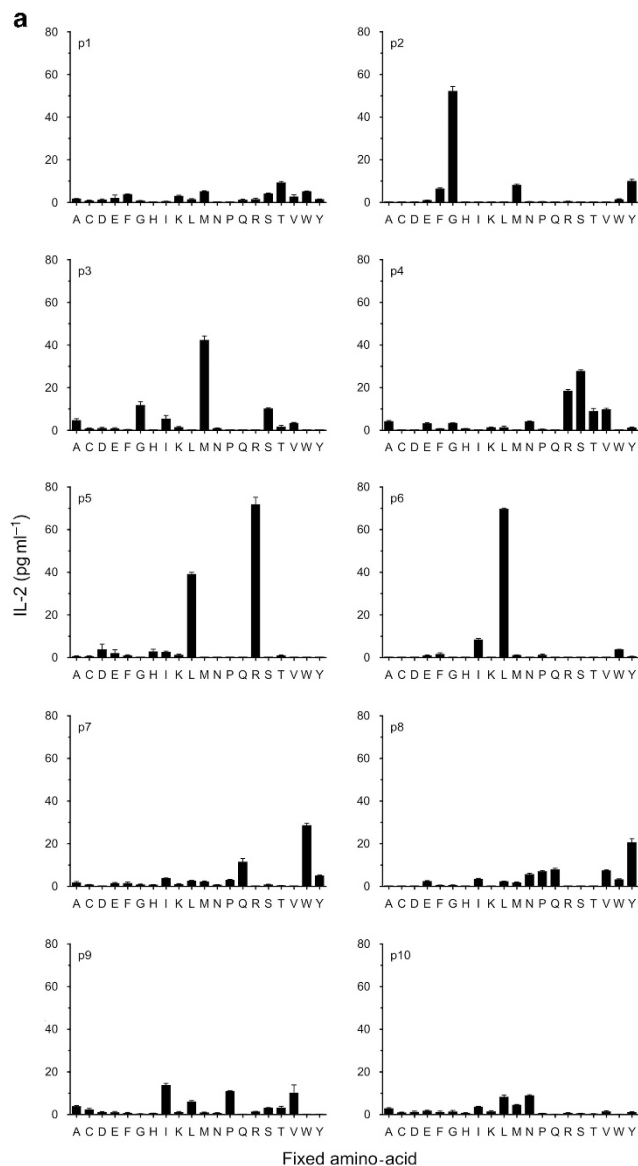
Fixed amino-acid

Net IL-2	Amino-acid position									
	1	2	3	4	5	6	7	8	9	10
>40 pg ml^{-1}		**G**	**M**		**R**	**L**				
20—40 pg ml^{-1}				**S**	**L**		**W**	**Y**		
10—20 pg ml^{-1}		Y	G	R				Q		I
			S							P
										V
5—10 pg ml^{-1}	**T**	M		V			Y	Q	L	L
	M			T				V		N
	W							P		
								N		

Figure 7 Response of T-cell transfectoma LB9-18 to 200 mixtures of decapeptide positional scanning library TPIMS 2040 in the presence of BeSO₄ (75 μM). (**a**) At each position of the peptide (p1–p10, see histograms), individual mixtures were composed of peptides having one defined amino-acid (20 amino acids, labeled on x axis in single letter code) and randomized amino acids at the remaining 9 peptide positions. T-cell transfectoma activation was assessed by interleukin (IL)-2 secretion (enzyme-linked immunosorbent assay) after overnight culture of transfectoma cells with mixtures (200 μg ml^{-1}) and BeSO₄, presented by DP2.21 cells in protein-free media. A positive IL-2 response to particular mixtures demonstrates the presence of active peptides within the mixture and provides insight into which amino acids are preferred at a given position of the peptide. Data show IL-2 (mean ± s.e.m.) of three separate experiments carried out in duplicate. IL-2 produced in wells not containing mixtures was below limits of detection. (**b**) Summary of the most active mixtures from positional scanning library TPIMS 2040. Mixtures were grouped by their ability to stimulate transfectoma LB9-18 by determining net IL-2 secretion (subtracting the amount of IL-2 secreted in wells not containing mixtures from IL-2 values obtained from wells that included mixtures). Bolded amino acids indicated those that were chosen for the generation of mimotopes.
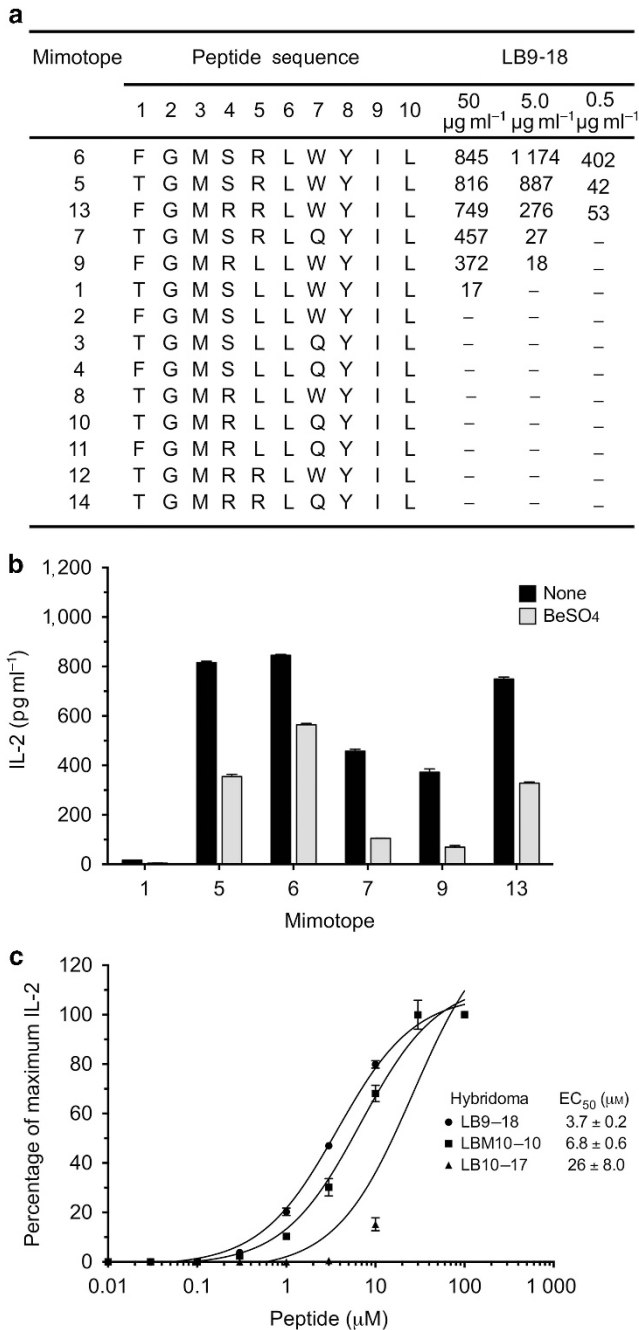
a

Mimotope	Peptide sequence										LB9-18 50 μg ml⁻¹	5.0 μg ml⁻¹	0.5 μg ml⁻¹
	1	2	3	4	5	6	7	8	9	10			
6	F	G	M	S	R	L	W	Y	I	L	845	1 174	402
5	T	G	M	S	R	L	W	Y	I	L	816	887	42
13	F	G	M	R	R	L	W	Y	I	L	749	276	53
7	T	G	M	S	R	L	Q	Y	I	L	457	27	–
9	F	G	M	R	L	L	W	Y	I	L	372	18	–
1	T	G	M	S	L	L	W	Y	I	L	17	–	–
2	F	G	M	S	L	L	W	Y	I	L	–	–	–
3	T	G	M	S	L	L	Q	Y	I	L	–	–	–
4	F	G	M	S	L	L	Q	Y	I	L	–	–	–
8	T	G	M	R	L	L	W	Y	I	L	–	–	–
10	T	G	M	R	L	L	Q	Y	I	L	–	–	–
11	F	G	M	R	L	L	Q	Y	I	L	–	–	–
12	T	G	M	R	R	L	W	Y	I	L	–	–	–
14	T	G	M	R	R	L	Q	Y	I	L	–	–	–

b

c

Figure 8 Beryllium (Be)-specific T-cell transfectomas recognize mimotopes in a beryllium (Be)-independent manner. (**a**) The sequence of each mimotope was based on the results of the decapeptide positional scanning for LB9-18. Equal numbers of LB9-18 cells and DP2.21 antigen-presenting cells were mixed with crude preparations of mimotopes (0.5, 5.0, and 50 μg ml⁻¹) and BeSO$_4$ (75 μM). Interleukin (IL)-2 secretion was measured by enzyme-linked immunosorbent assay after 22 h of culture. Mimotopes are ordered by LB9-18 response to 50 μg ml⁻¹ of peptide. Hyphens indicate no IL-2 secretion above background levels in response to mimotope. (**b**) T-cell transfectoma LB9-18 response to select mimotopes in the presence and absence of BeSO$_4$ (75 μM) is shown. Data are plotted as mean IL-2 secretion (pg ml⁻¹) for each mimotope. (**c**) Shown are dose–response curves for T-cell transfectomas LB9-18, LBM10-10, and LB10-17 to highly purified (>95%) mimotope 6 peptide. Data are plotted as the percentage of maximum IL-2 secretion against peptide. EC$_{50}$ values (μM) for each transfectoma are shown, and data are representative of three independent experiments.
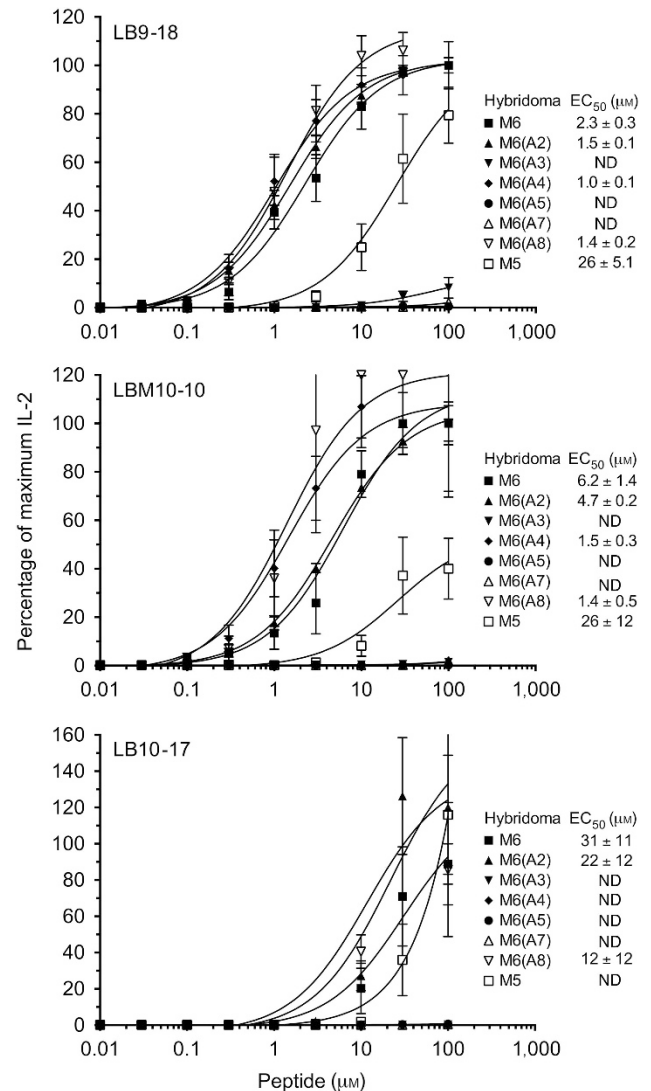

Figure 9 Beryllium (Be)-specific T-cell transfectoma response to alanine substitutions of mimotope 6. Peptide dose–response curves were completed for T-cell transfectomas LB9-18, LBM10-10, and LB10-17. Equal numbers of T-cell transfectoma cells and DP2.21 antigen-presenting cells were mixed with BeSO$_4$ (75 μM) and highly purified peptides with single alanine substitutions at positions 2, 3, 4, 5, 7, and 8 of mimotope 6. Interleukin (IL)-2 secretion was measured by enzyme-linked immunosorbent assay after 22 h of culture, and data are plotted as the percentage of maximum IL-2 secretion against peptide concentration in the presence of BeSO$_4$. EC$_{50}$ values (mean ± s.e.m., μM) for mimotope 6 and each variant peptide from four independent experiments are shown. ND, not determined.

The recently published structure of the HLA-DP2-mimotope 2/Be complex showed that binding of the Be^{2+} cation reduced the electrostatic surface potential and changed the surface topology of the HLA-DP2-peptide complex where the AV22 TCR Vβ CDR3 interacts.[29] Both of these changes must contribute to generation of the AV22 TCR ligand as this TCR is not stimulated by mimotope 2 without Be. In the absence of an HLA-DP2-mimotope 6 structure and insight into the actual Be-dependent epitope for the LB9-18 TCR, we can only speculate on how this Be-independent mimotope might imitate

the Be-specific TCR ligand. For example, the positively charged R at the p5 position of the peptide may substitute for Be^{2+} and reduce the electrostatic surface potential of the complex by partially neutralizing the solvent-exposed glutamic acids on HLA-DP2. In addition, the long side chain of R together with the bulky, hydrophobic W at p7 may create a conformation that mimics the conformation induced by the addition of Be^{2+} and Na^+ to the MHCII–endogenous peptide complex.[29] Of note, mutating E at positions 26, 68, and 69 of the HLA-DP2 β-chain abrogates Be-specific activation and IL-2 secretion of T-cell clones and transfectomas.[17,26,29] However, in the presence of Be-independent mimotope 6, fibroblasts expressing a variant HLA-DP2 molecule containing an isomorphic Q substitution at position 26 of the HLA-DP2 β-chain induced equivalent IL-2 secretion by the Be-specific T-cell transfectoma, LB9-18, compared with fibroblasts expressing native HLA-DP2. Thus our findings raise the possibility that the amino-acid composition of the Be-independent mimotopes mimics the charge and structural changes induced by the addition of Be^{2+} and Na^+ to the HLA-DP2-peptide complex.

Metal-independent mimotopes have been identified in other metal-induced hypersensitivities. For example, in subjects with nickel (Ni)-induced hypersensitivity, Ni-independent mimotopes were identified that replaced both the self-peptide and the Ni^{2+} ion bound to HLA-DR52c.[31] These mimotopes share a lysine (K) at the p7 position of the peptide. Structural analysis of a Ni-specific TCR interacting with the HLA-DR52c-peptide complex showed that the interface was dominated by TCR Vβ CDR3 interacting with the exposed p7 K.[31] These findings suggest that the Ni^{2+} cation directly contributes to the TCR interaction, which would contrast with the indirect effects of the Be^{2+} cation in altering both conformation and charge of HLA-DP2. Thus the Ni^{2+} and Be^{2+} cations may generate an adaptive immune response and metal-induced hypersensitivity via different mechanisms, with Ni^{2+} acting as a hapten and directly participating in TCR engagement while Be^{2+} indirectly induces a posttranslational alteration in an endogenous HLA-DP2-peptide complex. Collectively, these studies highlight the complexity of TCR recognition of metal-containing ligands.

When T cells derived from the site of pathology express the same Vβ and share a CDR3β motif, such as the Vβ6+ Be-specific TCRs investigated in the current study, it is usually inferred that these TCRs respond to the same antigen. Thus, although mimotope 6 was identified through an unbiased screen using the Be-specific T-cell transfectoma LB9-18, several of the other T-cell transfectomas were stimulated by this peptide. T-cell transfectomas LBM10-10 and LB10-17 responded to mimotope 6 presented by HLA-DP2 with varying affinities while LBM11-8 and LBM12-1 did not recognize it at all. LB9-18 and LBM10-10 recognized this MHCII–peptide complex with lower EC_{50} values compared with LB10-17. Thus, as the TCR β-chains of these three TCRs are identical, the differences in TCR affinity are due to the different α-chains expressed by these cells. In this regard, while both LB9-18 and LBM10-10 express Vα4 and Jα22, LB10-17 expresses Vα1 and

Jα45 and has a 5–10-fold higher EC_{50} than the other two Be-specific TCRs. In addition, the inability of LBM11-8 and LBM12-1 to respond to mimotope 6 likely stems from a combination of an R at position 95 of the TCR β-chain and expression of Vα1. Thus the response to mimotope 6 clearly relates to similarities of the recognizing TCRs (e.g., LB9-18 ≥ LBM10-10 > LB10-17 > > LBM11-8/LBM12-1).

In conjunction with characterizing the overall T-cell response to Be, we further analyzed murine-derived CD4+ T cells specific to the HLA-DP2-PLXNA4/Be complex, a T-cell specificity found in all HLA-DP2+ CBD subjects.[19] In the initial analysis, only 1 of the 29 Be-specific hybridomas stained with the Be-loaded HLA-DP2-PLXNA4 tetramer. Thus we confirmed our previous finding that these T cells are present in BeO-exposed HLA-DP2 Tg mice,[18] although they do not represent a major specificity. Further analysis of single-cell sorted tetramer-binding T cells enabled the identification of the TCR genes expressed by three additional T-cell clones. Two of these clones expressed homologous Vβ16+/Vα4+ TCRs that closely matched the sequence of the LBM10-13 TCR while the third clone expressed a completely unrelated Vβ6+ TCR. Similar to LBM10-13, none of these TCRs recognized the HLA-DP2-mimotope 2/Be tetramer. Thus tetramer co-staining patterns at the clonal level verified our previous findings of bulk BAL T cells derived from CBD patients.[19] In essence, subsets of T cells exist that either co-stain with mimotope 2 and plexin A4 tetramers or only bind to the tetramer presenting the endogenous antigen (plexin A4/Be). These differences likely reflect dissimilarities in TCR sequence among the antigen-specific population and are an important consideration when using a mimotope selected by a single TCR.

In the lungs of CBD patients, we previously identified Be-specific TCRs that were HLA-DP2-restricted, expressed nearly identical TCR Vβ5.1 chains while coupled with different TCR α-chains,[24] and comprised a public TCR repertoire.[25] Results in BeO-exposed HLA-DP2 Tg mice mirror what has been observed in human disease (i.e., identification of clonally expanded Vβ6+ Be-specific TCRs expressing identical or nearly identical β-chains coupled with differing TCR α-chains). These findings suggest that the Be-specific TCRs derived from both HLA-DP2-expressing mice and humans recognize the HLA-DP2-peptide/Be complex in a similar manner, with the majority of interactions contributed by TCR Vβ residues and the HLA-DP2 β1-chain.[29] These findings provide further validation for the use of the HLA-DP2 Tg murine model to study the initiation of a Be-specific adaptive immune response.

The identification of Be-independent mimotopes that mimic a Be-modified HLA-DP2-peptide complex raises the possibility that such peptides exist *in vivo* and can be involved in the maintenance of the Be-specific T-cell response. We found, however, that CD4+ T cells derived from the lungs of BeO-exposed HLA-DP2 Tg mice and Be-specific CD4+ T-cell lines derived from CBD patients do not secrete interferon-γ or IL-2 in response to the Be-independent mimotope 6 (data not shown). In addition, preliminary experiments studying adoptively transferred Vβ6+ CD4+ T cells derived from the lungs

of BeO-exposed HLA-DP2 Tg mice showed that this cell population failed to preferentially home to or expand in recipient lungs compared with spleen in the absence of BeO exposure (data not shown). Collectively, these data suggest that T cells reactive to these Be-independent mimotopes do not exist *in vivo*. It is likely that the persistent inflammation seen in HLA-DP2-expressing mice and CBD patients is secondary to persistent antigen exposure as Be remains within lung granulomas for decades after the cessation of exposure.[32]

In conclusion, the present work identifies Be-independent mimotopes for a set of oligoclonal TCRs derived from the lungs of BeO-exposed HLA-DP2 Tg mice. The utilization of highly related TCR β-chains paired with different α-chains suggests that TCR interactions with the Be antigen are dominated by the TCR β-chain, regardless of species. Although the Be-independent mimotopes likely do not have *in vivo* relevance, they further our understanding of Be-induced alterations in the topology of the HLA-DP2-peptide complex. Future studies utilizing TCR Tg mice expressing HLA-DP2-plexin A4/Be or Vβ6 Be-specific TCRs will enable us to define mechanisms of disease pathogenesis. Thus HLA-DP2 Tg mice provide a powerful tool for the dissection of the role of Be-specific CD4^{+} T cells in the generation of Be-induced hypersensitivity.

METHODS

Exposure of mice to Be and preparation of lung cells. HLA-DP2 (*HLA-DPA1*0103* and *-DPB1*0201*) Tg mice on an FVB/N background were generated as previously described.[18,33] Mice were bred and maintained in the Biological Resource Center at the University of Colorado Denver in accordance with the National Institutes of Health guidelines for use of live animals. All experiments were conducted with the approval of the Institutional Animal Care and Use Committee of the University of Colorado Denver.

Six-to-8-week-old HLA-DP2 Tg FVB/N mice were anesthetized with isoflurane, and 100 μg BeO (NIST, standard reference material 1877) was administered via oropharyngeal aspiration on days 0, 1, 2, 14, 15, 18, and 19.[18] Mice were killed on day 21, and single-cell suspensions of splenocytes were prepared.[18] Harvested lungs were minced and digested in tissue culture medium containing 1 mg ml^{−1} collagenase (Sigma-Aldrich, St Louis, MO). After 30 min at 37 °C, digested lung tissue was disrupted, and the lung cells were centrifuged. After lysis of erythrocytes, lung cells were filtered through a 70-μM cell strainer and resuspended in complete tumor media, consisting of Minimum Essential Medium, 10% fetal bovine serum, and 6% tumor cocktail as previously described.[34] Collection of BAL cells was performed by three successive intratracheal instillations of 0.5 ml phosphate-buffered saline.

Generation of Be-specific T-cell hybridomas. Be-specific T-cell hybridomas were generated as previously described.[35] In brief, lung cell suspensions from 10 mice were pooled and restimulated *in vitro* at 2×10^6 ml^{−1} with 10 μM BeSO$_4$ in complete tumor media. After 4 days in culture, T-cell blasts were enriched by density gradient centrifugation (Histopaque, Sigma-Aldrich) and expanded in IL-2 for 3 days. T-cell hybridomas were established by fusion of T cells to TCR α[−]/β[−] BW5147 thymoma cells using polyethylene glycol and cloned by limiting dilution under hypoxanthine, aminopterin, and thymidine (Invitrogen, Life Technologies, Grand Island, NY) selection. T-cell hybridoma clones were screened for Be specificity by measuring IL-2 production by enzyme-linked immunosorbent assay (eBioscience, San Diego, CA) after stimulation with 200 μM BeSO$_4$ presented by an HLA-DP2-transfected murine fibroblast, designated DP8302.

Determination of *TCRA* and *TCRB* gene usage. To determine *TCRB* gene usage, total RNA was isolated using a Qiagen RNeasy Kit (Qiagen, Valencia, CA), and cDNA was prepared as previously described.[14] *TCRB* gene fragments were PCR-amplified using a 3′ *TCRBC* primer and a panel of BV primers (n = 13) to screen for *TCRBV* gene usage of each of the hybridomas. An identical PCR screening methodology was employed to determine *TCRAV* gene segment usage, using a 3′ *TCRAC* primer and panel of AV primers (n = 22). Upon determination of specific *BV* and *AV* gene segment usage, larger-scale PCR reactions were completed, and products were purified using a DNA binding membrane spin column (Qiagen) and sequenced (Applied Biosystems, Carlsbad, CA).

Transfectomas expressing particular murine Be-specific TCRs. Because T-cell hybridomas created by fusing murine T cells with BW5147 cells are tetraploid and genetically unstable, TCRs expressed by select Be-specific hybridomas were cloned into expression vectors and stably transfected into the mouse hybridoma cell line 54ζ, which expresses human CD4,[19,24,25,36] as described in the **Online Supplement**.

Decapeptide positional scanning library and peptide synthesis. The decapeptide library used for this study (designated TPIMS 2040) is a synthetic *N*-acetylated, C-terminal amidated, L-amino-acid combinatorial peptide library organized in a positional scanning format. This library consists of 200 mixtures prepared in an OX9 format where O represents a specific amino-acid at a defined position and X represents an equimolar mixture of all natural amino acids (except cysteine) in each of the remaining 9 positions. Each OX9 mixture consists of 3.2×10^{11} different decapeptides, and the total number of peptides in the library is 6.4×10^{12}.[22,37] T-cell transfectoma response to HLA-DP2-expressing fibroblasts presenting peptide mixtures in the presence of Be was assessed by IL-2 secretion. The amount of IL-2 secreted in wells not containing mixtures was subtracted from IL-2 values obtained from wells that included mixtures to yield net IL-2 (pg ml^{−1}).

Individual candidate peptides (mimotopes), selected based on analysis of positional scanning results, were synthesized using the PEPScreen 96-well array (Sigma). Peptides chosen for further studies were synthesized on a larger scale and tested at 95% purity (CPC Scientific, Sunnyvale, CA). All peptides were first dissolved in dimethyl sulfoxide at high concentration prior to making a working stock in phosphate-buffered saline.

HLA-DP2-PLXNA4/Be tetramer staining and cell sorting. Preparation of soluble, Be-loaded HLA-DP2-covalent plexin A4 peptide (PLXNA4) tetramers was performed as previously described.[19] For sorting of HLA-DP2 tetramer-binding CD4^{+} T cells, lung cells ($5\text{-}10 \times 10^6$ cells per mouse) from BeO-exposed HLA-DP2 Tg FVB/N mice were incubated in 25 μl of medium containing 5 μM sodium azide, an excess of FcR-specific blocking monoclonal antibody (mAb), and the phycoerythrin-labeled HLA-DP2-PLXNA4/Be tetramer (20 μg ml^{−1}). After 2 h at 37 °C, fluorescently conjugated mAbs to murine CD3 (PE-Cy7), CD4 (AF700), CD11c (APC-eFluor 780), B220 (eFluor 450), F4/80 (eFluor 450), CD8 (eFluor 450), and CD44 (PerCP-Cy5.5) were added, and cells were incubated at 4 °C an additional 30 min. After washing, cells were analyzed on a FACSAria flow cytometer (BD Immunocytometry Systems, San Jose, CA). Cells staining with mAbs directed against B220, F4/80, CD8, and CD11c were included in a dump gate and excluded from analysis. Using forward and side scatter patterns, dump-negative, CD3^{+}CD4^{+} T cells were selected and sorted based on tetramer staining and high CD44 expression.

Cloning of PLXNA4/Be-specific TCRs from CD4^{+} T cells isolated by single-cell sorting. A single-cell suspension was prepared from the lungs of BeO-exposed HLA-DP2 Tg mice as described previously.[18] Cells were stained with mAbs directed against CD4 (AF700), CD3 (PE-Cy7), CD8 (eFluor 450), B220 (eFluor 450), F4/80 (eFluor 450),

CD44 (PerCP-Cy5.5), and phycoerythrin-labeled HLA-DP2-PLXNA4/Be tetramer.[19] Tetramer$^+$CD3$^+$CD4$^+$CD44$^+$ T cells were single cell sorted into reverse transcription buffer in a 96-well plate using a FACSAria flow cytometer. *TCRAV* and *TCRBV* gene expression was determined using 5′ rapid amplification of cDNA ends and a nested PCR method as previously described[25,38] and as detailed in the **Online Supplement**.

SUPPLEMENTARY MATERIAL is linked to the online version of the paper at http://www.nature.com/mi

REFERENCES
1. Richeldi, L., Sorrentino, R. & Saltini, C. HLA-DPB1 glutamate 69: a genetic marker of beryllium disease. *Science* **262**, 242–244 (1993).
2. Richeldi, L. *et al.* Interaction of genetic and exposure factors in the prevalence of berylliosis. *Am. J. Ind. Med.* **32**, 337–340 (1997).
3. Wang, Z. *et al.* Differential susceptibilities to chronic beryllium disease contributed by different Glu69 HLA-DPB1 and -DPA1 alleles. *J. Immunol.* **163**, 1647–1653 (1999).
4. Rossman, M.D. *et al.* Human leukocyte antigen Class II amino acid epitopes: susceptibility and progression markers for beryllium hypersensitivity. *Am. J. Respir. Crit. Care Med.* **165**, 788–794 (2002).
5. Maier, L.A. *et al.* Influence of MHC class II in susceptibility to beryllium sensitization and chronic beryllium disease. *J. Immunol.* **171**, 6910–6918 (2003).
6. McCanlies, E.C., Ensey, J.S., Schuler, C.R., Kreiss, K. & Weston, A. The association between HLA-DPB1Glu69 and chronic beryllium disease and beryllium sensitization. *Am. J. Ind. Med.* **46**, 95–103 (2004).
7. Van Dyke, M.V. *et al.* Risk of chronic beryllium disease by HLA-DPB1 E69 genotype and beryllium exposure in nuclear workers. *Am. J. Respir. Crit. Care Med.* **183**, 1680–1688 (2011).
8. Kreiss, K., Mroz, M.M., Newman, L.S., Martyny, J. & Zhen, B. Machining risk of beryllium disease and sensitization with median exposures below 2mg/m³. *Am. J. Ind. Med.* **30**, 16–25 (1996).
9. Kreiss, K., Mroz, M.M., Zhen, B., Martyny, J.W. & Newman, L.S. Epidemiology of beryllium sensitization and disease in nuclear workers. *Am. Rev. Respir. Dis.* **148**, 985–991 (1993).
10. Kreiss, K., Wasserman, S., Mroz, M.M. & Newman, L.S. Beryllium disease screening in the ceramics industry: blood test performance and exposure-disease relations. *J. Occup. Med.* **35**, 267–274 (1993).
11. Fontenot, A.P., Canavera, S.J., Gharavi, L., Newman, L.S. & Kotzin, B.L. Target organ localization of memory CD4$^+$ T cells in patients with chronic beryllium disease. *J. Clin. Invest.* **110**, 1473–1482 (2002).
12. Fontenot, A.P. *et al.* CD28 costimulation independence of target organ versus circulating memory antigen-specific CD4$^+$ T cells. *J. Clin. Invest.* **112**, 776–784 (2003).
13. Fontenot, A.P. *et al.* Frequency of beryllium-specific, central memory CD4$^+$ T cells in blood determines proliferative response. *J. Clin. Invest.* **115**, 2886–2893 (2005).
14. Fontenot, A.P., Falta, M.T., Freed, B.M., Newman, L.S. & Kotzin, B.L. Identification of pathogenic T cells in patients with beryllium-induced lung disease. *J. Immunol.* **163**, 1019–1026 (1999).
15. Fontenot, A.P., Kotzin, B.L., Comment, C.E. & Newman, L.S. Expansions of T-cell subsets expressing particular T cell receptor variable regions in chronic beryllium disease. *Am. J. Respir. Cell Mol. Biol.* **18**, 581–589 (1998).
16. Fontenot, A.P., Torres, M., Marshall, W.H., Newman, L.S. & Kotzin, B.L. Beryllium presentation to CD4$^+$ T cells underlies disease susceptibility HLA-DP alleles in chronic beryllium disease. *Proc. Natl. Acad. Sci. USA* **97**, 12717–12722 (2000).
17. Lombardi, G. *et al.* HLA-DP allele-specific T cell responses to beryllium account for DP-associated susceptibility to chronic beryllium disease. *J. Immunol.* **166**, 3549–3555 (2001).
18. Mack, D.G. *et al.* Regulatory T cells modulate granulomatous inflammation in an HLA-DP2 transgenic murine model of beryllium-induced disease. *Proc. Natl. Acad. Sci. USA* **111**, 8553–8558 (2014).
19. Falta, M.T. *et al.* Identification of beryllium-dependent peptides recognized by CD4$^+$ T cells in chronic beryllium disease. *J. Exp. Med.* **210**, 1403–1418 (2013).
20. Hemmer, B. *et al.* The use of soluble synthetic peptide combinatorial libraries to determine antigen recognition of T cells. *J. Pept. Res.* **52**, 338–345 (1998).
21. Pinilla, C., Appel, J.R., Blanc, P. & Houghten, R.A. Rapid identification of high affinity peptide ligands using positional scanning synthetic peptide combinatorial libraries. *Biotechniques* **13**, 901–905 (1992).
22. Pinilla, C., Appel, J.R. & Houghten, R.A. Investigation of antigen-antibody interactions using a soluble, non-support-bound synthetic decapeptide library composed of four trillion (4×10^{12}) sequences. *Biochem. J.* **301**, 847–853 (1994).
23. Osman, G.E. *et al.* FVB/N (H2(q)) mouse is resistant to arthritis induction and exhibits a genomic deletion of T-cell receptor V beta gene segments. *Immunogenetics* **49**, 851–859 (1999).
24. Bowerman, N.A., Falta, M.T., Mack, D.G., Kappler, J.W. & Fontenot, A.P. Mutagenesis of beryllium-specific TCRs suggests an unusual binding topology for antigen recognition. *J. Immunol.* **187**, 3694–3703 (2011).
25. Bowerman, N.A. *et al.* Identification of multiple public T cell receptor repertoires in chronic beryllium disease. *J. Immunol.* **192**, 4571–4580 (2014).
26. Bill, J.R. *et al.* Beryllium presentation to CD4$^+$ T cells is dependent on a single amino acid residue of the MHC class II β-chain. *J. Immunol.* **175**, 7029–7037 (2005).
27. Dai, S. *et al.* Crystal structure of HLA-DP2: Implications for chronic beryllium disease. *Proc. Natl. Acad. Sci. USA* **107**, 7425–7430 (2010).
28. Sidney, J. *et al.* Five HLA-DP molecules frequently expressed in the worldwide human population share a common HLA supertypic binding specificity. *J. Immunol.* **184**, 2492–2503 (2010).
29. Clayton, G.M. *et al.* Structural basis of chronic beryllium disease: linking allergic hypersensitivity and autoimmunity. *Cell* **158**, 132–142 (2014).
30. Fontenot, A.P. & Maier, L.A. Genetic susceptibility and immune-mediated destruction in beryllium-induced disease. *Trends Immunol.* **26**, 543–549 (2005).
31. Yin, L., Crawford, F., Marrack, P., Kappler, J.W. & Dai, S. T-cell receptor (TCR) interaction with peptides that mimic nickel offers insight into nickel contact allergy. *Proc. Natl. Acad. Sci. USA* **109**, 18517–18522 (2012).
32. Sawyer, R.T., Abraham, J.L., Daniloff, E. & Newman, L.S. Secondary ion mass spectroscopy demonstrates retention of beryllium in chronic beryllium disease granulomas. *J. Occup. Environ. Med.* **47**, 1218–1226 (2005).
33. Tarantino-Hutchison, L.M. *et al.* Genetic determinants of sensitivity to beryllium in mice. *J. Immunotoxicol.* **6**, 130–135 (2009).
34. Kappler, J.W., Skidmore, B., White, J. & Marrack, P. Antigen-inducible, H-2-restricted, interleukin-2 producing T cell hybridomas: lack of independent antigen and H-2 recognition. *J. Exp. Med.* **153**, 1198 (1981).
35. Ignatowicz, L., Kappler, J. & Marrack, P. The repertoire of T cells shaped by a single MHC/peptide ligand. *Cell* **84**, 521–529 (1996).
36. Boen, E., Crownover, A.R., McIlhaney, M., Korman, A.J. & Bill, J. Identification of T cell ligands in a library of peptides covalently attached to HLA-DR4. *J. Immunol.* **165**, 2040–2047 (2000).
37. Hemmer, B. *et al.* Identification of candidate T-cell epitopes and molecular mimics in chronic Lyme disease. *Nat. Med.* **5**, 1375–1382 (1999).
38. Ozawa, T., Tajiri, K., Kishi, H. & Muraguchi, A. Comprehensive analysis of the functional TCR repertoire at the single-cell level. *Biochem. Biophys. Res. Commun.* **367**, 820–825 (2008).
39. Arden, B., Clark, S.P., Kabelitz, D. & Mak, T.W. Mouse T-cell receptor variable gene segment families. *Immunogenetics* **42**, 501–530 (1995).